Separation Science and Technology
Publication details, including instructions for authors and subscription information:
http://www.informaworld.com/smpp/title~content=t713708471

On-Line Coupling of Thermal Field-Flow Fractionation with Low-Angle Laser Light Scattering

Michel Martin[a]; Jan Hes[b]
[a] LABORATOIRE DE CHIMIE ANALYTIQUE PHYSIQUE, ECOLE POLYTECHNIQUE, PALAISEAU, FRANCE [b] DIONEX CORPORATION, SUNNYVALE, CALIFORNIA

To cite this Article Martin, Michel and Hes, Jan(1984) 'On-Line Coupling of Thermal Field-Flow Fractionation with Low-Angle Laser Light Scattering', Separation Science and Technology, 19: 10, 685 — 707
To link to this Article: DOI: 10.1080/01496398408060669
URL: http://dx.doi.org/10.1080/01496398408060669

SEPARATION SCIENCE AND TECHNOLOGY, **19**(10), pp. 685-707, 1984

On-Line Coupling of Thermal Field-Flow Fractionation with Low-Angle Laser Light Scattering*

MICHEL MARTIN

LABORATOIRE DE CHIMIE ANALYTIQUE PHYSIQUE
ECOLE POLYTECHNIQUE
91128 PALAISEAU, FRANCE

JAN HES

DIONEX CORPORATION
SUNNYVALE, CALIFORNIA 94086

Abstract

The analysis of a polymethyl methacrylate sample dissolved in dimethylformamide is performed by using a low-angle laser light scattering photometer attached to a thermal field-flow fractionation channel and a differential refractometer. Relevant theoretical light scattering equations for flow-through operation are outlined. It is shown that the calibration curve of the separation system can be constructed *in situ* during the course of separation, without using any calibration standard. The average molecular weights as well as the molecular weight distribution curves of the polymer have been determined. The sensitivity of the light-scattering photometer has been measured, and it is compared to that of the differential refractometer in terms of signal-to-noise ratios. The various sources of errors in the molecular weight determination are discussed, and the potential of the coupling for physicochemical studies on the thermal diffusion of polymers is indicated. In spite of some inherent problems, this coupling is expected to have a very bright future if reliable low-angle light-scattering instruments can be made available at moderate prices.

INTRODUCTION

Thermal field-flow fractionation is one of the subclasses of field-flow fractionation (FFF) in which a temperature gradient is used to induce a

*Part of this paper was presented at the 13th International Symposium on Chromatography, Cannes, France, June 30–July 4, 1980.

 0149-6395/84/1910-0685$3.50/0

nonuniform concentration distribution of a given species in the various velocity streamlines of the flow in an open rectangular channel. Species having different concentration profiles migrate at different velocities along the channel and eventually become separated at the outlet where they are detected (*1*).

The interplay of the transverse concentration and velocity profiles on the axial sample migration velocity has been theoretically investigated (*2*) and experimentally studied in thermal FFF using polystyrene standards with narrow molecular weight distributions (*3*). It is now well established that the retention of these samples in thermal FFF depends chiefly on their thermal diffusion factors, which has been shown to increase steadily with the molecular weight of the polymer (*2*). Consequently, thermal FFF separates a polymer sample according to the molecular weights of its constituents. The selectivity of thermal FFF for the polystyrene samples appears to be several times larger than that of gel permeation chromatography (*4*). The primary factors affecting the sample peak broadening have been recognized (*5, 6*) and can be controlled to achieve high efficiencies so that the overall fractionation power of thermal FFF overcomes that of any current polymer separation technique (*4*). Accordingly, present thermal FFF systems have peak capacities in the range 10–50 (*7*).

Besides these intrinsic advantages, thermal FFF is a versatile technique. It can be made fast; separations in minutes or less have been achieved (*8*). The temperature gradient can be externally programmed so that adequate resolution can be achieved over the whole retention spectrum of polymers with a broad molecular weight range (*9*). Pressurizing the channel extends the temperature range over which the eluent is liquid. This allows low molecular weight samples to be satisfactorily resolved by using a large temperature drop between the hot and cold plates (*10*). This also permits to use the "cold" (that is, lower temperature) plate at high temperature in order to meet solubility requirements of poorly soluble polymers, like polyolefins (*11*).

Orienting the channel vertically with the injection point at the bottom allows one to take advantage of the thermogravitational effect for adjusting the velocity profile and improving the resolution of low molecular weight polymers or of other species having weak thermal diffusion factors (*13*). Up to now, thermal FFF has been shown to be successfully applicable to different types of polymers including, besides polystyrene, polytetrahydrofuran (*14*), polyisoprene (*14*), polymethyl methacrylate (*13, 14*) and polyethylene (*11*). However, it has consistently failed, up to now, to adequately retain, and thus separate, polymers soluble in aqueous solutions (*3, 15*).

It seems, in light of recent theoretical predictions (*16, 17*) and from a survey of available data on thermal diffusion (*13*), that polyelectrolytes have fairly low thermal diffusion coefficients. However, a detailed theory of thermal diffusion in solutions (Soret effect) is still lacking. This is one of the major reasons why the applications of thermal FFF have been so limited up to now, in spite of its great separation potential and its inherent advantages described above. Indeed, since it is not possible to predict the thermal diffusion coefficient of a given polymer, the feasibility of its thermal FFF analysis and the operating conditions (solvent and temperature gradient) have to be experimentally determined by trial-and-error successive assays. More importantly, since it is not possible to *a priori* relate the thermal diffusion factor, which determines the retention, with the molecular weight of a given polymer type, one needs, in order to derive the molecular weight distribution (MWD) curve of an unknown sample from its thermal FFF elution spectrum, to obtain the calibration curve of this particular polymer type. This determination is similarly required for the interpretation of steric exclusion chromatography (gel permeation chromatography) data and can be obtained by observing the retention behavior of several narrowly dispersed standards or of a broadly dispersed standard of the same chemical structure as the sample, with known MWD, or by using the so-called universal calibration procedure, which allows one to use the standards with chemical structures different from that of the sample (*18*). Unfortunately, no such universal calibration scheme, which hinges on a correct description of the retention mechanism, can be used in thermal FFF, because no theory can satisfactorily describe the dependence of thermal diffusion on the polymer chemical structure in terms of available parameters. Therefore, when a satisfying separation can be obtained by thermal FFF, it cannot be interpreted in terms of MWD if the sample does not belong to the rather small number of polymer types for which standards are available.

Calibration curves are required to relate the amount of polymer at a given elution volume to its molecular weight. This amount of polymer is usually determined by a classical concentration detector (UV or IR photometer, differential refractometer, fluorometer, etc.). If other possibilities do exist to establish the correspondence between elution volume and molecular weight, then calibration curves are no longer required prior to separation. One such possibility is to use a molecular weight detector (that is, a detector giving a signal depending on the molecular weight of the macromolecules present in its cell at a given time) in a sufficiently simple way so that this molecular weight (or an average one) can be extracted from the signal. Such molecular weight detectors have to be found among the techniques classically used for measuring average molecular weights of polymers, such as osmometry, or

methods based on the colligative properties of solutions, diffusion, ultracentrifugation, birefringence, etc. However, in order to be compatible with the separation performances of thermal FFF (or steric exclusion chromatography), the techniques of polymer characterization must be amenable to the following requirements: they must have flow-through cells of small volumes, their response time must be fast, and they must have high sensitivity. Up to now, two molecular weight detectors satisfying these requirements have been adapted to elution separation techniques. One is a continuous viscometer, which hinges on application of the Mark-Houwink relationship between the intrinsic viscosity of a polymer and its molecular weight (*19*). The second one is a light-scattering detector. In the following, we describe the coupling of such a detector with a thermal FFF channel. First, the basic characteristics of light scattering are presented.

THEORY OF LIGHT SCATTERING FROM POLYMER SOLUTIONS

The theory of light scattering from polymer solutions and colloidal suspensions has a long history and includes notable contributions from Maxwell, Tyndall, Rayleigh, Lorenz, Einstein, Smoluchowski, Mie, Debye, Gans, and many others (*20, 21*).

When a beam of light is directed at a solution of polymers, some of the light is transmitted unperturbed through the solution, some may be absorbed, and some is scattered. Light scattering is associated with oscillations of the electron clouds of the atoms induced by the interaction of the oscillating electric field of the incident light, and, more generally, with any source of nonuniformity in a medium, like density fluctuations induced by thermal motions in a liquid phase. Basically, light scattering is measured in terms of the Rayleigh factor, R_θ:

$$R_\theta = I_\theta r^2/(I_0 V) \tag{1}$$

where I_θ is the intensity of the scattered light at angle θ from the forward direction of the incident beam and at distance r from the scattering source, I_0 is the intensity of the incident beam, and V is the scattering volume which is simultaneously illuminated and viewed by the detector. As the scattered light is frequently measured by optoelectronic devices, such as photomultiplier tubes, which sense radiant power (or flux) rather than light intensity, one alternative, and more practical, definition of R_θ is

$$R_\theta = (P_\theta/P_0)(1/\sigma l) \tag{2}$$

where P_θ and P_0 are the scattered and incident power, respectively, σ is the solid angle of the detected scattered beam, and l is the length, parallel to the incident beam, of the scattering volume.

In a polymer solution there is, in addition to the scattering of the pure solvent, another contribution arising from the concentration fluctuations of the polymer in the solution. This contribution leads to the definition of the excess Rayleigh factor, $\bar{R}_\theta$, which is of utmost importance in the present context, since it contains informations related to the polymer solute:

$$\bar{R}_\theta = R_{\theta,\,\text{solution}} - R_{\theta,\,\text{solvent}} \tag{3}$$

For a very dilute solution of macromolecules of a size small in comparison with the wavelength of the incident beam, $\bar{R}_\theta$ can be expressed, for unpolarized light and isotropic polymer molecules, as

$$\bar{R}_\theta = 2\pi^2 n^2 (dn/dc)^2 cM(1 + \cos^2\theta)/(\lambda_0^4 N_A) \tag{4}$$

where λ_0 is the wavelength *in vacuo* of the incident light, n is the refractive index of the solution (or, in practice, of the solvent, as the solution is dilute), c is the weight concentration of the solute of molecular weight M, and N_A is Avogadro's number. Equation (4) can be rewritten as

$$\bar{R}_\theta = KcM \tag{5}$$

where K is the optical constant:

$$K = 2\pi^2 n^2 (dn/dc)^2 (1 + \cos^2\theta)/\lambda_0^4 N_A \tag{6}$$

For a polydisperse polymer solution with a weight concentration c_i of molecules with molecular weight M_i, the overall intensity of scattered light is the sum of the intensities of light scattered by each species M_i:

$$\bar{R}_{\theta,\text{tot}} = \sum_i R_{\theta,\,i} \tag{7}$$

where, according to Eq. (5):

$$\bar{R}_{\theta,i} = Kc_i M_i \tag{8}$$

The average molecular weight, $\bar{M}$, measured by the light-scattering technique, is

$$\bar{M} = \bar{R}_{\theta,\text{tot}}/(Kc_{\text{tot}}) \tag{9}$$

with

$$c_{tot} = \sum_i c_i \tag{10}$$

The combination of Eqs. (7) to (10) gives

$$\bar{M} = \sum_i c_i M_i / \sum_i c_i \tag{11}$$

Noting that

$$c_i = N_i M_i / V \tag{12}$$

where N_i is the number of macromolecules with molecular weight M_i in solution of volume V, one has

$$\bar{M} = \sum_i N_i M_i^2 / \sum_i N_i M_i \tag{13}$$

Therefore, the average molecular weight obtained by light scattering is a weight average, M_w.

When the concentration of the solution is such that interactions between the macromolecules reduce the amplitude of local fluctuations of solute concentration due to thermal motion, the intensity of scattered light is also reduced. Then, the expression of the excess Rayleigh factor is corrected by introduction of a term containing the virial coefficients of the osmotic pressure equation, as they reflect these interactions:

$$\bar{R}_\theta = KcM/(1 + 2A_2cM + 3A_3c^2M + \cdots) \tag{14}$$

Moreover, when the size of the macromolecules become larger than about $\lambda/20$, where λ is the wavelength of the radiation in the solution, destructive interferences between waves scattered by different parts of the molecule will further reduce the amount of scattered light. For example, in the case of polystyrene molecules dissolved in benzene, illuminated by the red light of a helium-neon laser, this occurs when the molecular weight is larger than about 70,000 daltons. Accordingly, a multiplicative correction factor, $P(\theta)$, the value of which is lower than 1, is introduced in Eq. (14) to account for these interferences. This factor depends on the size and on the shape of the macromolecules and is, for this reason, called the form factor. In addition, it depends on the angle θ. However, as the scattering angle becomes smaller and smaller, the phase differences between scattered waves coming from different parts of the molecule become smaller and smaller, and, therefore, $P(\theta)$ becomes closer to 1. It has been shown (*21*) that, whatever the shape of the molecule, the limiting expression of $P(\theta)$ for small θ can be written

$$P(\theta) = 1 - (16\pi^2 R_g^2 \sin^2(\theta/2)/3\lambda^2) \quad (15)$$

where R_g is the radius of gyration of the molecules, which also depends on the concentration. It can be calculated that, in the case of polystyrene in benzene with a He-Ne laser source, $P(\theta)$ will be larger than 0.99 if the molecular weight is smaller than 6.8×10^5 daltons when θ equals 20°. This limiting molecular weight becomes 1.8×10^5 and 7.2×10^6 daltons when θ equals 45 and 5°, respectively. Therefore, because the MWD of real world polymers is usually wide, and a significant part of the sample molecules have molecular weights extending well beyond 10^6 daltons, accurate measurements of the weight-average molecular weight cannot be done by neglecting the $P(\theta)$ correction to Eq. (14), unless measurements are made at a fairly low scattering angle (less than about 5°). This is the reason why classical light-scattering measurements, which cannot be carried out at such small angles, require considerable work with double extrapolation to zero scattering angle and zero concentration to draw the so-called Zimm diagrams. Such a technique is obviously not amenable to the requirements for thermal FFF detectors mentioned above.

However, the recent introduction of laser technology in light scattering as well as in various photometric methods allows the measurement of the intensity of the scattered light to be made at a very low angle, lower than 5° (*22–24*). The laser beam, indeed, can be focused on a very small area, where the Gaussian power distribution within the beam produces a large scattering response from a small volume (about 0.1 μL). This low-angle laser light-scattering (LALLS) photometer can therefore fulfill the requirements for a thermal FFF detector. In addition, such a small scattering volume minimizes the problems usually encountered with dust particles in light-scattering measurements.

Therefore, with the LALLS photometer, the form factor can be safely assumed equal to 1 for most polymer solutions which do not contain an appreciable amount of macromolecules with gyration radii larger than about 0.2–0.5 μm. From the signal of the LALLS photometer, which is proportional to $\bar{R}_\theta$, one can under these conditions determine the product cM of the weight concentration and the molecular weight of the polymer present in the cell at a given time. Neglecting the third- and higher-order virial coefficients in Eq. (14) gives the following expression:

$$cM = 1/((K/\bar{R}_\theta) - 2A_2) \quad (16)$$

which, if $A_2 cM \ll 1$, can be simplified to

$$cM = \bar{R}_\theta / K \quad (17)$$

The signal from the concentration-sensitive detector, placed in series with the LALLS detector, is proportional to c. Therefore, provided that the sample concentration is not significantly modified in the transfer line from one detector to the other one, the values of c and M can both be determined as a function of the elution volume. The practical method of construction of the desired MWD consists in determining the values of c and M at a certain number of locations along the elution curves of the two detectors. This method and others used for determination of the various average molecular weights from the elution curves have been described elsewhere (*25*) and can be applied for any separation technique (i.e., for instance, thermal FFF as well as steric exclusion chromatography). These methods rely on the basic relationship between the elution curve of the concentration sensitive detector, $c(V_R)$, where V_R is the elution (or retention) volume and the normalized MWD curve, $w(M)$:

$$w(M) = c(V_R)\,|dV_R/dM|/m \tag{18}$$

where m is the mass of sample injected. This equation expresses that the weight fraction of sample with molecular weights included in the range from M to $M + dM$ is equal to the weight fraction of the sample eluting between V_R and $V_R + dV_R$. When the c and M values are determined at uniform retention volume intervals, the weight-average and number-average molecular weights, M_w and M_n, respectively, are given by (*25*)

$$M_w = \sum_i c_i M_i / \sum_i c_i \tag{19}$$

and

$$M_n = \sum_i c_i / \sum_i (c_i/M_i) \tag{20}$$

the sums extending to all locations where c_i and M_i have been determined.

EXPERIMENTAL

The schematic diagram of the apparatus used in this study is shown in Fig. 1. It consists of three parts: feeding system, separation channel, and detection system.

A dual-piston, high-pressure Model 6000 A reciprocating pump from Waters Associates (Milford, Massachusetts) is used to deliver the eluent to the system. The solvent, dimethylformamide (DMF), obtained from Prolabo (Paris, France), flows through a used 30 cm long, 7 mm i.d. liquid

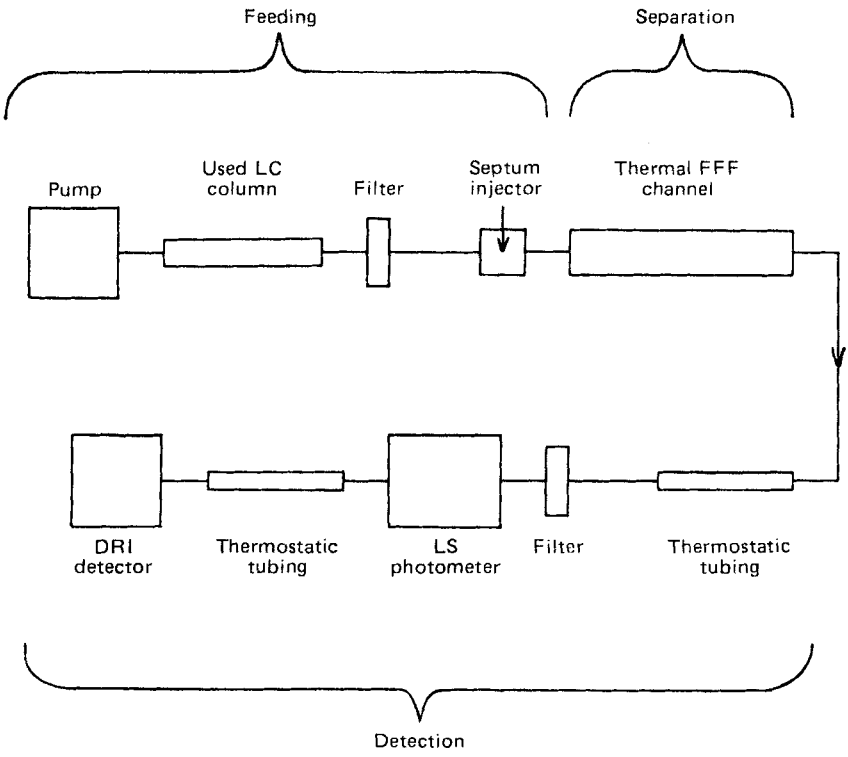

FIG. 1. Schematic diagram of the apparatus assembly.

chromatographic column, packed with 10 μm particles, which is used to provide a high back pressure for proper operation of the pump at the selected flow rate of 0.2 mL/min, as well as to act as a relatively large primary and gross filtering unit for the eluent and as a device for damping the residual flow and pressure pulsations of the pump. A filter unit containing a PTFE disk membrane filter with a 0.2-μm nominal pore size (Type FG from Millipore, Bedford, Massachusetts) is inserted between the LC column and the thermal FFF channel in order to eliminate the larger particulate contaminants of the eluent.

The thermal FFF channel has been previously described (*13*). The rectangular cross-section channel, cut into a Mylar sheet, is 0.1 mm thick, 2.05 cm wide, and 41.6 cm long. A polymethyl methacrylate (PMMA) sample, obtained from Polysciences (Warrington, Pennsylvania), was used, namely PMMA 160 ($M_w = 160{,}000$, $M_w/M_n < 1.1$). A 10-μL sample of solution of PMMA in DMF was introduced in a silicone-septum injector

with a Hamilton, no. 701 syringe. The concentration of the injected solution was 1.553 g/mL. The temperature drop between the two plates was 34°C and the cold plate temperature was 23°C.

The effluent of the FFF channel flows through the detection system which is made up of the light-scattering photometer and a concentration-sensitive detector placed in series. A differential refractometer (Model R 401 from Waters Associates) is used to monitor the weight concentration of the channel effluent. Because the cell of this detector cannot withstand pressures larger than about 5 bars, this detector is placed downstream of the other one, so that its outlet is at nearly atmospheric pressure. In order to obtain a homogeneous solution temperature in the cell of the LALLS photometer, a 75 cm long, 0.23 mm i.d. thermally insulated capillary tubing is used to connect it to the channel outlet. Another capillary tubing of the same dimensions allows the connection of the outlet of the light-scattering detector with the inlet port of the differential refractive index (DRI) detector. It has been found necessary to insert a filter unit, similar to the one described above, just upstream of the LALLS photometer, in order to reduce the amount of particles present in the channel effluent. In spite of a rather large dead volume, mainly due to the filter unit, between the channel and the DRI detector, the peak profile of the polymer was not found significantly different than when this detector is directly connected to the channel outlet.

The light-scattering detector, Model KMX-6 from Chromatix (Sunnyvale, California), is equipped with a 10-μL cell with a 5-mm optical path clamped between two thick silica windows. The light of a helium-neon laser (wavelength in vacuo: 632.8 nm) is focused on the center of the flow cell and the scattered light passing through an annulus, whose axis coincides with the direction of the incident beam, is collected by means of a relay lens onto a photomultiplier tube. The signal of this tube is sent to a potentiometric recorder. When no sample is eluting from the channel, the signal corresponding to the scattering of the pure eluent is recorded as a stable baseline. The excess scattering due to the sample is thus measured from this baseline. In the present study the annulus selected corresponds to an average scattering angle of 4.54° and a solid angle of 5.84 msr.

RESULTS AND DISCUSSION

In spite of the care taken to filter the eluent, the signal from the LALLS photometer contains numerous spikes due to the passage of particles in the light beam. However, because of the small scattering volume (0.1 μL) inside the cell, the residence time of each particle in the beam is much shorter than the time of elution of the polymer sample peak. At the selected flow rate of

0.2 mL/min, the transit time of a particle in the beam is about 30 ms. Therefore the duration of a spike on the recorder is of the order of magnitude of the response time of the detector and recorder assembly. Consequently, it is not difficult to eliminate the contribution of the spikes to the signal manually and obtain the sample elution curve (fractogram) from the LALLS photometer with a minimal loss of precision. Such a curve is shown in Fig. 2 together with the peak recorded from the DRI signal. The scales of the two signals are indicated in terms of the basic units of measurement of the detectors, that is, RI units for the differential refractometer and cm^{-1}, the CGS unit of Rayleigh excess factor, for the LALLS detector. The volume of solvent eluting from the channel during the occurrence of a peak signal from both detectors is about 3 mL.

The data of the two curves were manually processed by measurements of the peak heights of the two signals at 30 locations 0.1 mL apart along the two curves. The concentration at a given location was deduced from the peak height, y_{RI}, of the DRI detector, as

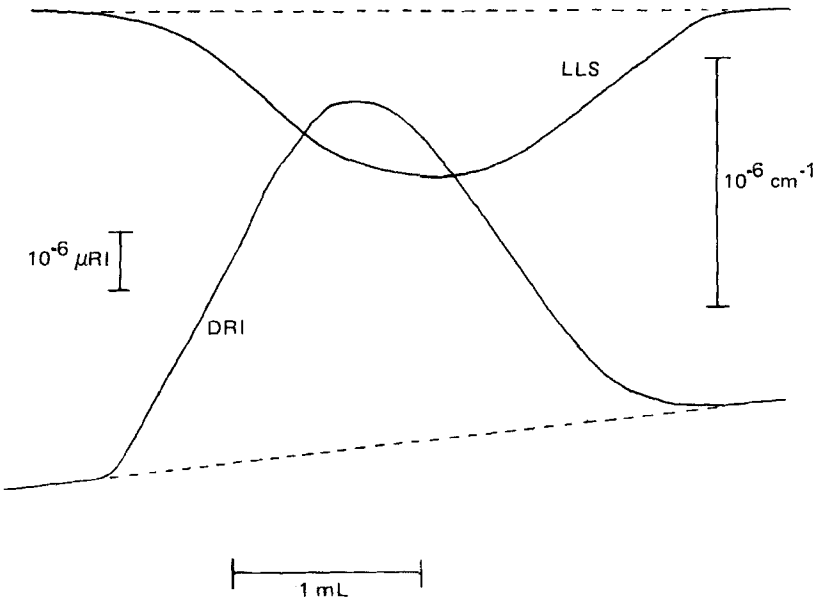

FIG. 2. Elution curves of the PMMA 160 sample from the thermal FFF channel obtained from the laser light-scattering (LLS) photometer (upper curve) and from the differential refractometer (lower curve). See the text for the experimental conditions.

$$c = y_{RI}/k_{RI} \tag{21}$$

where k_{RI} is a proportionality constant determined as:

$$k_{RI} = AF/(mv_p) \tag{22}$$

where A is the area included between the DRI baseline and the DRI curve (in mm^2), F is the flow rate (in mL/min), m is the amount of sample injected (in g), and v_p is the chart speed (in mm/min).

The signal, in mV, of the LALLS detector, measured on the recorder from the baseline, is proportional to the excess radiant power of the scattered beam, $\bar{P}_\theta$. This signal, y_{LS}, can be written as

$$y_{LS} = S_a \bar{P}_\theta T \tag{23}$$

where S_a is the anode sensitivity of the detector and T is the transmittance of the optical system for the scattered beam. In order to determine the excess Rayleigh factor, it is necessary to measure the radiant power of the incident beam, P_0. Generally, P_0 is usually 10^6 times larger than the total radiant power scattered in all directions. Therefore, P_0 can be estimated from the measurement of the radiant power of the transmitted beam, with a completely negligible error. With the instrument used, this is done by replacing the annulus by a small diameter diaphragm, so the transmittance of the optical system for the transmitted beam is the same as for the scattered beam. However, because the intensity of the transmitted light is about 10^8–10^9 larger than the intensity of the scattered light beam at low angle, it is necessary, in order to avoid damage of the photomultiplier tube, to insert several optical attenuators of appropriate overall transmittance, D, in the path of the incident beam. The detector signal for the transmitted beam, y_0, which can be read either on the chart recorder or on the digital indicator of the instrument, is then equal to

$$y_0 = S_a P_0 TD \tag{24}$$

The excess Rayleigh factor at each location on the fractogram is then equal, according to Eqs. (2) and (3), to

$$\tilde{R}_\theta = (y_{LS}/y_0)(D/\sigma l) \tag{25}$$

The transmittance of each attenuator can be separately measured with the instrument and their product, D, determined. The σl value depends on the scattering angle and solid angle selected, on the optical arrangement of the

system, and on the refractive index of the solution (solvent), and is determined from data tabulated in the instruction manual. Proper operation of the LALLS detector requires, of course, that y_0 does not change appreciably during the course of a thermal FFF run, which implies good stability of the laser source. In order to determine the product cM from y_{LS}, using Eq. (16), one must know the value of the virial coefficient A_2 and evaluate the optical constant K, from Eq. (6). The specific refractive index increment, dn/dc, has been taken as 0.0619 mL/g, a value given for isotactic PMMA in DMF at 20°C and at a wavelength of 644 nm (*26*). The refractive index, n, of the DMF eluent has been selected as its n_D^{20} value, 1.4305 (*26*). Although the wavelength of the sodium yellow D line (589.3 nm) differs from that of the helium-neon laser (632.8 nm), the error introduced by using this value is assumed to be small. Indeed, the relative variation of the refractive index between these two wavelengths for typical organic solvents is about 0.1–0.3% (*27*). The second virial coefficient, A_2, has been taken as equal to 6×10^{-4} mol·mL/g^2 (*26*).

For each of the 30 locations along the elution curves, the c and cM values, as well as their ratio M, were determined from the signals of the DRI and LALLS detectors, respectively, according to Eq. (21) for c and Eqs. (25), (16), and (6) for cM. The calibration curve, $V_R(M)$, can then be constructed without the need of any standard. The curve is shown in Fig. 3. As expected

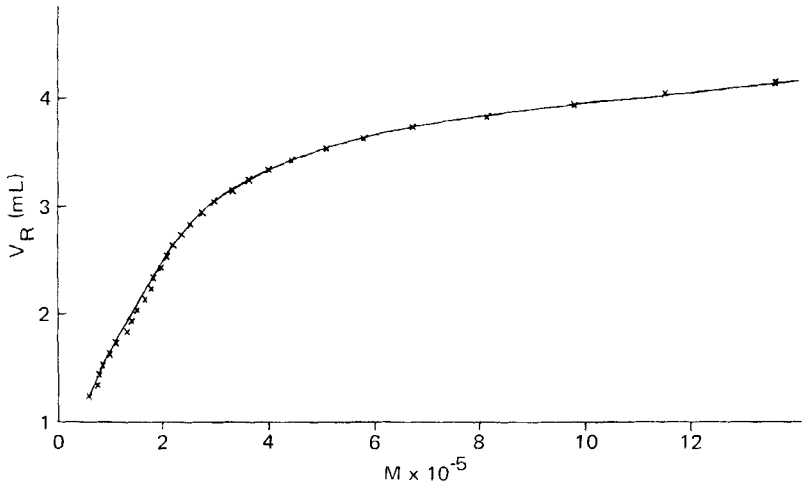

FIG. 3. Calibration curve for PMMA in DMF determined from the coupling of the LALLS and DRI detectors without using any standards. Temperature drop between the two plates: 34°C. Cold plate temperature: 23°C.

from previous retention observations with polystyrene standards, it confirms that the retention volume in thermal FFF increases with increasing molecular weights of the polymer. It is noteworthy that, in spite of the crude manual procedure used to build this curve, the molecular weight value determined for each value of the retention volume is always larger than the molecular weights corresponding to lower values of V_R. From the curve, the derivative, dV_R/dM can be measured for each V_R value more accurately than successive values of $\Delta V_R/\Delta M$, since the curve smoothes the errors associated with successive determinations of M. This derivative is then used in combination with the c value at each point and the amount of polymer injected, m, to calculate the probability density of the MWD curve by weight, $w(M)$, according to Eq. (18). The resulting normalized MWD curve by weight is shown in Fig. 4. The weight-average molecular weight, M_w, can then be determined as the first moment of this curve. However, it can be more conveniently calculated from each of thirty cM and c values according to Eq. (19). This value is found to be equal to 249,500 daltons. It is significantly larger than the stated nominal value for the PMMA sample, which is 160,000.

The density probability function of the MWD curve by number, $f(M)$, can easily be calculated from $w(M)$ as

$$f(M) = M_n w(M)/M \tag{26}$$

The number-average molecular weight, M_n, is equal, according to Eq. (20) to 194,600 daltons. The polydispersity index, which is the ratio of M_w to M_n, is equal to 1.28. It is larger than the value stated by the manufacturer (<1.1). The reason for this is not clear. However, a rather large value of this index has already been found for a similar sample from the intercept of the plate height curve (*13*). The normalized MWD curve by number, $f(M)$, is shown in Fig. 5. The curve appears to be relatively sharply peaked at M equal to about 150,000. The shape of this curve is rather unusual. It is not clear if the steep slope of the curve at low molecular weights reflects the true distribution or if it is an artifact due to the inaccuracy of the measurements in this molecular weight range. Indeed, it has already been noted, in the combination of the light scattering detector with steric exclusion chromatography, that measurements are inaccurate in both ends of the elution curves. In the lower M range the signal of the LALLS detector, which is proportional to M, is small and may be masked by the baseline noise. In the upper M range the LALLS signal may still be measured while the DRI signal vanishes, leading to very large M values.

This is a rather general problem occurring in the combination of the LALLS detector with a separation method. It results in loss of accuracy in

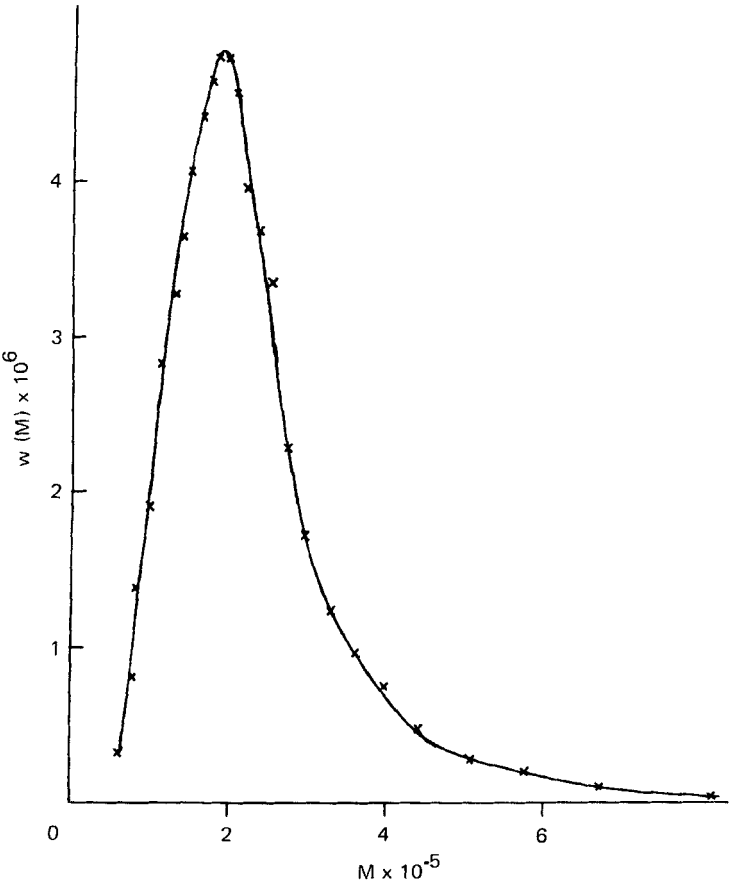

FIG. 4. Normalized molecular weight distribution curve by weight of PMMA 160.

the measurement of the MWD curves as well as of the average molecular weights, since when one of the two signals becomes too small, the molecular weight calculated from the determination of cM and c becomes either infinite or zero. However, one may suggest the following method for minimizing the associated errors. As discussed above, in the intermediate retention volume interval where the signals of both detectors are accurately measurable, the calibration curve may be constructed. One can then extrapolate this curve to both ends of the elution curves by any appropriate means (manually or by use of a computer program) and use this extrapolated curve in the low M region, where c can be measured from the concentration-sensitive detector signal, to determine M, and in the high M region, where cM can be measured

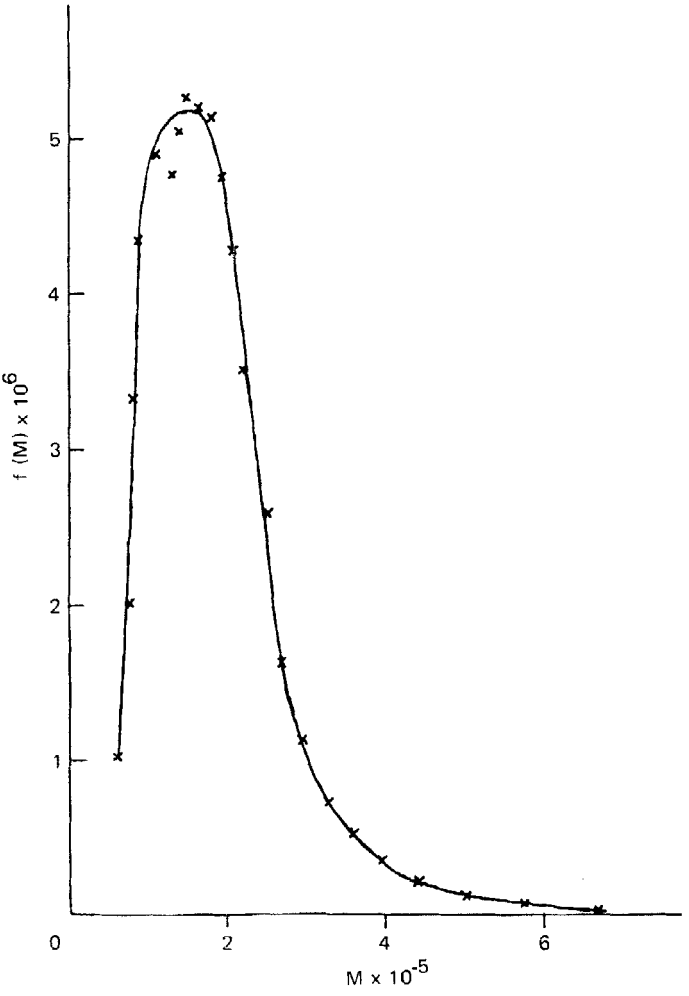

FIG. 5. Normalized molecular weight distribution curve by number of PMMA 160.

from the LALLS detector signal, to determine c. Then these additional couples of c and M data can be included in the above-described methods for determination of the average molecular weights and the MWD curves with improved accuracy.

In addition to the above-mentioned problem, the precision of the measurements at the low M end of the MWD curve, which corresponds to V_R values close to the channel void volume, may be reduced by the fact that a negative peak appears with the DRI detector at the void volume. This sometimes occurs in thermal FFF, especially with highly hygroscopic solvents, like DMF. Nevertheless, the calibration curve plotted in Fig. 3 can be used to relate the basic FFF dimensionless parameter λ, which is the ratio of the space constant of the exponential concentration distribution of the solute in the direction of the thermal gradient to the channel thickness (l), to the molecular weight M. λ is calculated from V_R as the solution of

$$6\lambda\mathscr{L}(1/2\lambda) = V_0/V_R \tag{27}$$

where V_0 is the channel void volume and $\mathscr{L}(x)$ is the Langevin function (*8*). Although this retention equation, which is based on a parabolic velocity profile assumption, is not exact for thermal FFF since distortion of the flow profile occurs because of the temperature dependence of the solvent viscosity, the level of precision of the measurements does not necessitate the use of a more accurate relationship between λ and V_R. In Fig. 6, λ is plotted versus M on a log-log scale. Surprisingly, this plot is not linear on the full M range covered by the sample from about 60,000 to 1,300,000 daltons. This is in contradistinction with previous findings for polystyrene samples. A linear plot would be expected if the thermal diffusion coefficient does not depend on M while the molecular coefficient is inversely proportional to M^a (*13*). For polystyrene, it has been found that a is equal to about 0.55–0.6, in agreement with modern theories of polymer solutions in good solvents. The linear regression analysis of the data in Fig. 6 for M lower than about 300,000 gives an a value of 0.77, which seems to be rather large if it is to be attributed only to the variation of the molecular diffusion coefficients with the molecular weight of the polymer. Clearly, more work is needed to elucidate this point and show if this large a value is due to a molecular weight dependence of the thermal diffusion coefficient or to the limited precision of the measurements. At high M values, however, a is found to have a rather low value of about 0.2.

Nevertheless, the curve in Fig. 6 shows that the LALLS photometer combined with the thermal FFF channel can provide a means of investigating the retention mechanism of this separation technique. At this point it is interesting to give a figure of the sensitivity of the light-scattering photometer.

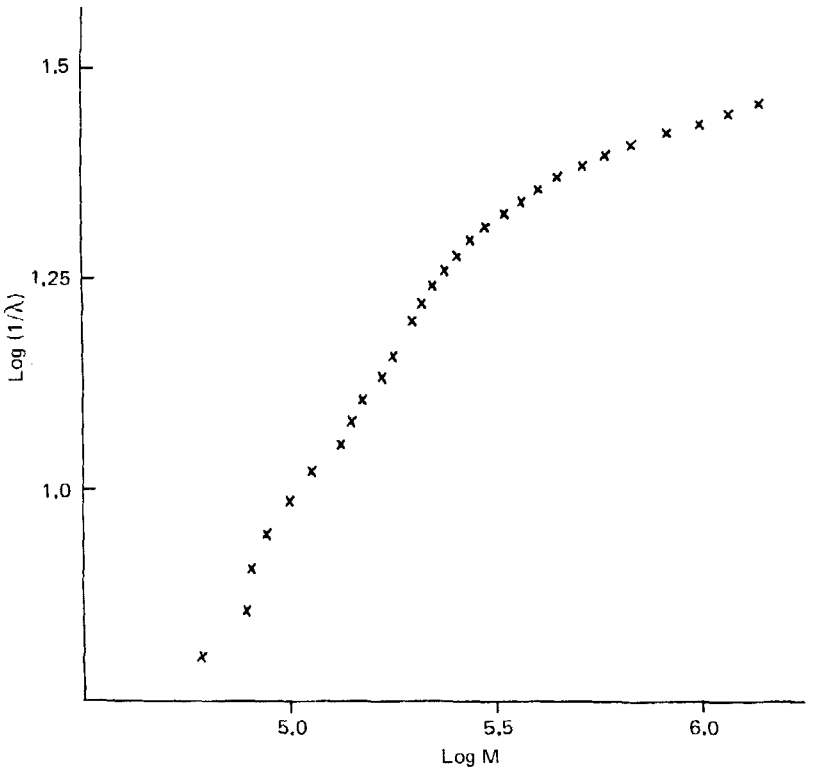

FIG. 6. Plot of λ vs M on a log-log scale for the PMMA sample. Same experimental conditions as for Fig. 3.

Let N_{LS} be the noise of the LALLS detector, in cm^{-1}, the CGS unit of Rayleigh excess factor. Then the limit of detection of the detector, which is some multiple, k ($k = 2$, 5, or 10, depending on the arbitrary convention chosen), of the noise level, obviously depends on the molecular weight of the sample according to equations developed in the theoretical section. It can be expressed from Eq. (5) as

$$c_{\min,LS} = kN_{LS}/KM \tag{28}$$

The noise level experimentally observed in flow-through conditions with the LALLS detector corresponds to an excess Rayleigh factor of 4×10^{-8} cm^{-1}.

Numerical calculations for the He-Ne laser with a scattering angle of 5° and a polymer–solvent system such that n and dn/dc equal 1.5 RIu and 0.1 mL g, respectively, show that, if $k = 2$ and $M = 10^5$, the limit of detection, which is the minimal detectable concentration at the channel outlet (or more precisely, in the LALLS cell) is equal to 8.7×10^{-6} g/mL. This concentration is highly sensitive to the value of dn/dc as this quantity is squared in the expression of K. It may be interesting to compare the sensitivity of the LALLS photometer to that of the DRI detector. In the following, suffixes LS and RI refer to the light scattering and refractive index detectors, respectively. Let r_{LS} and r_{RI} be the signal-to-noise ratios for these two detectors. In the high dilution operating conditions of most elution zonal separation techniques, one has

$$r_{RI} = c(dn/dc)/N_{RI} \tag{29}$$

and

$$r_{LS} = K_0 n^2 (dn/dc)^2 cM/N_{LS} \tag{30}$$

with

$$K = K_0 n^2 (dn/dc)^2 \tag{31}$$

K_0 is an optical constant of the LALLS photometer, which does not depend on the polymer–solvent system. It is equal to 4.07×10^{-6} CGSu under present experimental conditions. The ratio of the signal-to-noise ratio is then

$$r_{LS}/r_{RI} = (N_{RI}/N_{LS}) K_0 n^2 (dn/dc) M \tag{32}$$

This ratio depends on the noise ratio. Under the present experimental conditions, the noise level of the DRI detector has been found to be about 4×10^{-7} RIu. In the case of PMMA dissolved in DMF, it appears that the signal-to-noise ratio of the LALLS detector is larger than the corresponding ratio of the DRI detector when M is larger than about 194,000 daltons and vice versa. This critical M value is lower for larger dn/dc values. It is also sensitive to the exact value of the solvent refractive index, but to a lesser extent, although n is squared in Eq. (32), because n^2 does not change much more than 15% from one solvent to another.

CONCLUSION

In the combination of the low-angle laser light-scattering photometer with a thermal FFF channel and a concentration sensitive detector (here, differential refractometer) for the determination of the calibration curve, $V_R(M)$, of the separator, and, hence, of the molecular weight distribution curve of the polymer, there are numerous sources of errors. First of all, the values of the specific refractive index increment of the polymer, dn/dc, and of the second virial coefficient must be provided. The accuracy of the dn/dc value is particularly critical as the signal of the LALLS detector is nearly proportional to the square of this parameter. Moreover, this value must be determined at the wavelength of the laser light. Unfortunately, tabulated values are usually not given at the He-Ne laser wavelength and extrapolations must frequently be done. One should note, however, that, when the dn/dc value at this wavelength cannot be found or directly measured, it can, in some circumstances, be obtained from static measurements of the light scattered by the polymer (*28*). The dn/dc and A_2 values must not appreciably depend on the molecular weight or, if it is not the case, this dependence must be known. In addition, the k_{RI} proportionality coefficient in Eq. (21) must not depend on M, which is generally valid when M exceeds about 10,000. On the other end, the signal of the LALLS photometer must effectively be due to the light scattered by the sample. This excludes operation with samples which exhibit fluorescence at the wavelength of the laser. Although the selection of a red source does limit the occurrence of this phenomenon, some samples cannot be used, such as asphaltenes, for example.

Besides, the concentration versus time profile of the polymer sample must not be distorted in the transfer line between the LALLS and DRI detectors. In fact, band broadening always occurs in the connection tube, which must be small compared to the overall width of the sample peak. In addition, the delay time due to the transfer of sample between the two cells must be precisely known so that the two detector signals can be adequately related. Furthermore, this delay time must not vary with the molecular weight in order, first, to avoid distortion of the concentration peak and, second, to properly correlate the detector signals. Problems linked with such a variation have been noted (*29*). While the reason for this is not entirely clear, it may be due, at least in part, to hydrodynamic effects (pressure drop between the two cells larger at large M or steric exclusion of large molecules from the capillary walls, although these two effects act oppositely).

The equations developed above for determination of the MWD curve, especially Eq. (18), assume that a precise relationship can be established between the elution volume and the molecular weight. However, macromolecules of a given M elute at varying elution volumes because of the band

broadening in the separation process. It should be taken into account for proper evaluation of the MWD curve. However, this requires knowledge of the elution curve of a monomolecular species and its variation with the species molecular weight. This results in considerable complexity, necessitating the use of a computer. For this reason, this band broadening correction was generally not made until the recent advent of dedicated microcomputers. It should be noted that errors associated with the neglect of this correction are expected to be smaller in thermal FFF than in steric exclusion chromatography, because of the larger fractionation power of the FFF technique. Anyway, the value of M_w determined from Eq. (19) is expected to be more accurate than other average molecular weights, since the LALLS detector basically measures a weight-average molecular weight.

However, in spite of these various sources of errors, the potential of the coupling of thermal FFF with the LALLS photometer appears very great. Indeed, the present experimental study shows that such a coupling can be made to work. It can relieve one of the major obstacles which have limited the extension of the thermal FFF technique, in spite of its inherent advantages described in this introduction: the construction of the calibration curve for the particular polymer–solvent system under study is no longer required prior to the analysis since such a curve can be obtained *in situ* during the course of the separation. This extends the possibility of applications of thermal FFF to many polymer samples for which suitable calibration standards are not available. One should note that, once the calibration curve has been determined for a given solvent–polymer type system and a given temperature, subsequent analyses of unknown samples of this polymer under the same experimental conditions (solvent, temperatures of the plates) do not require the use of the LALLS detector and can be done with a simple experimental arrangement including only a concentration sensitive detector downstream of the channel. The MWD curve is then determined according to Eq. (18).

Furthermore, as shown for the study of the PMMA sample, the relationship between the basic FFF parameter, λ, which, in the case of thermal FFF, is directly related to the thermal diffusion factor, and the molecular weight can be determined. In addition, this determination can be made, for a given polymer, in various solvents at different values of the temperature gradient and/or of the average temperature. Consequently, this coupling of thermal FFF with the LALLS technique is a powerful tool for the physicochemical study of the thermal diffusion of polymers. Particularly, the dependence or independence of the thermal diffusion coefficient, which is the migration velocity induced by the temperature drop per unit value of the thermal gradient, on the molecular weight could be elucidated by this means. In turn, by a feedback effect, such physicochemical studies should help to

develop semiempirical useful expressions for the optimization of the thermal FFF process.

Consequently, the work performed here on a PMMA sample dissolved in DMF, using the coupling of a thermal FFF channel and a LALLS photometer, is a preliminary study showing the feasibility of this coupling and indicating its potential. It is hoped that, in the future, reliable and moderately priced LALLS instruments will be developed and will become commercially available.

Acknowledgments

The assistance of Dr Luis Saintout in the experimental work is greatly acknowledged. Samples were prepared by Dr René Reynaud.

REFERENCES

1. M. E. Hovingh, G. H. Thompson, and J. C. Giddings, *Anal. Chem., 42* 195 (1970).
2. J. C. Giddings, *J. Chem. Phys., 49*, 81 (1968).
3. M. N. Myers, K. D. Caldwell, and J. C. Giddings, *Sep. Sci., 9*, 47 (1974).
4. J. C. Giddings, Y. H. Yoon, and M. N. Myers, *Anal. Chem., 47*, 126 (1975).
5. L. K. Smith, M. N. Myers, and J. C. Giddings, *Ibid., 49*, 1750 (1977).
6. M. Martin, M. N. Myers, and J. C. Giddings, *J. Liq. Chromatogr., 2*, 147 (1979).
7. M. Martin and A. Jaulmes, *Sep. Sci. Technol., 16*, 691 (1981).
8. J. C. Giddings, M. Martin, and M. N. Myers, *J. Chromatogr., 158*, 419 (1978).
9. J. C. Giddings, L. K. Smith, and M. N. Myers, *Anal. Chem., 48*, 1587 (1976).
10. J. C. Giddings, L. K. Smith, and M. N. Myers, *Ibid., 47*, 2389 (1975).
11. S. L. Brimhall, M. N. Myers, K. D. Caldwell, and J. C. Giddings, *Sep. Sci. Technol., 16*, 671 (1981).
12. J. C. Giddings, M. Martin, and M. N. Myers, *Ibid., 14*, 611 (1979).
13. M. Martin and R. Reynaud, *Anal. Chem., 52*, 2293 (1980).
14. J. C. Giddings, M. N. Myers, and J. Janca, *J. Chromatogr., 186*, 37 (1979).
15. J. C. Giddings, K. D. Caldwell, and M. N. Myers, *Macromolecules, 9* 106 (1976).
16. F. Brochard and M. Martin, *Bull. Soc. Fr. Phys., 46*, 17 (1982).
17. F. Brochard-Wyart, *Macromolecules, 16*, 149 (1983).
18. J. Janca, in *Advances in Chromatography*, Vol. 19 (J. C. Giddings, E. Grushka, J. Cazes, and P. R. Brown, eds.), Dekker, New York, 1981, Chap. 2.
19. A. C. Ouano, *J. Polym. Sci., Polym. Chem. Ed., 10*, 2169 (1972).
20. M. Kerker, *The Scattering of Light and Other Electromagnetic Radiation*, Academic, New York, 1969.
21. M. B. Huglin (ed.), *Light Scattering from Polymer Solutions*, Academic, New York, 1972.
22. W. Kaye, A. J. Havlik, and J. B. McDaniel, *J. Polym. Sci., Part B, 9*, 695 (1971).
23. W. Kaye, *Anal. Chem., 45*, 221A (1973).
24. W. Kaye and A. J. Havlik, *Appl. Opt., 12*, 541 (1973).
25. M. Martin, *Chromatographia, 15*, 426 (1982).

26. J. Brandup and E. H. Immergut (eds.), *Polymer Handbook*, 2nd ed., Wiley, New York, 1975.
27. P. W. Atkins, *Physical Chemistry*, 2nd ed., Freeman, San Francisco, 1982.
28. M. Martin, Unpublished Results.
29. J. G. Bindels, Personal Communication.